Developmental Biology 334 (2009) 345–354

Contents lists available at ScienceDirect

Developmental Biology

journal homepage: www.elsevier.com/developmentalbiology

The *ADAXIALIZED LEAF1* gene functions in leaf and embryonic pattern formation in rice

Ken-ichiro Hibara [a,1], Mari Obara [a,1], Emi Hayashida [a,2], Masashi Abe [a], Tsutomu Ishimaru [a,3], Hikaru Satoh [b], Jun-ichi Itoh [a], Yasuo Nagato [a,*]

[a] *Graduate School of Agricultural and Life Sciences, University of Tokyo, Tokyo 113-8657, Japan*
[b] *Institute of Genetic Resources, Faculty of Agriculture, Kyushu University, Fukuoka 812-8581, Japan*

ARTICLE INFO

Article history:
Received for publication 23 March 2009
Revised 9 July 2009
Accepted 20 July 2009
Available online 6 August 2009

Keywords:
ADAXIALIZED LEAF1 (*ADL1*)
Phytocalpain
Adaxial–abaxial axis
Embryo development
Aleurone layer
Epidermis specification

ABSTRACT

The adaxial–abaxial axis in leaf primordia is thought to be established first and is necessary for the expansion of the leaf lamina along the mediolateral axis. To understand axis information in leaf development, we isolated the *adaxialized leaf1* (*adl1*) mutant in rice, which forms abaxially rolled leaves. *adl1* leaves are covered with bulliform-like cells, which are normally distributed only on the adaxial surface. An *adl1* double mutant with the *adaxially snowy leaf* mutant, which has albino cells that specifically appear in the abaxial mesophyll tissue, indicated that *adl1* leaves show adaxialization in both epidermal and mesophyll tissues. The expression of *HD-ZIPIII* genes in *adl1* mutant increased in mature leaves, but not in the young primordia or the SAM. This indicated that *ADL1* may not be directly involved in determining initial leaf polarity, but rather is associated with the maintenance of axis information. *ADL1* encodes a plant-specific calpain-like cysteine proteinase orthologous to maize *DEFECTIVE KERNEL1*. Furthermore, we identified intermediate and strong alleles of the *adl1* mutant that generate shootless embryos and globular-arrested embryos with aleurone layer loss, respectively. We propose that *ADL1* plays an important role in pattern formation of the leaf and embryo by promoting proper epidermal development.

Introduction

Leaves are determinate organs that serve as the main photosynthetic organ in plants. Leaf primordia start from the cells recruited from the peripheral zone of the shoot apical meristem (SAM), and their development progresses precisely along the proximodistal, mediolateral, and adaxial–abaxial axes. The establishment of these axes is an important step in plant development, and many genetic and molecular biological studies suggest that the formation of each axis is regulated independently (Bowman et al., 2002; Chitwood et al., 2007). Among these three axes, adaxial–abaxial patterning occurs at the earliest stage of leaf development, and subsequent lamina outgrowth is triggered at the juxtaposition of adaxial and abaxial domains (Waites and Hudson, 1995; Reinhardt et al., 2005). Surgical isolation of leaf primordia from the SAM via excision or laser ablation results in abaxialized leaves (Sussex, 1951; Reinhard et al., 2005). This suggests that a meristem-borne signal confers adaxial identity to incipient primordia.

Members of the Class III *HD-Zip* gene family contribute to establishing continuity from the SAM to the adaxial domain of leaf primordia. The *REVOLUTA* (*REV*), *PHABULOSA* (*PHB*), and *PHAVOLUTA* (*PHV*) (REV clade) genes in this class appear to play an important role in the establishment of the SAM and adaxial identity of the lateral organs. Although loss-of-function mutations in *PHB* and *PHV* result in nearly normal phenotypes, the *phb phv rev* triple mutant shows a single abaxialized cotyledon and lacks the embryonic SAM (Emery et al., 2003; Prigge et al., 2005). REV clade genes are expressed in both the adaxial domain of the leaf primordium and the adjacent region of the SAM. This polarized expression pattern results from post-transcriptional gene silencing in the abaxial leaf domain by miRNA 165/166 and *KANADI* genes, which also have an antagonistic function as abaxial identity genes (Reinhart et al., 2002; Rhoades et al., 2002; Tang et al., 2003; Eshed et al., 2004). Dominant gain-of-function mutations in these Class III *HD-Zip* genes, which show mutations in miRNA recognition sites in *Arabidopsis*, result in adaxialized leaf polarity (McConnell and Barton, 1998; McConnell et al., 2001; Emery et al., 2003; Zhong and Ye, 2004; Ochando et al., 2006). Despite the developmental differences between monocot and dicot leaves, the spatial regulation of REV clade gene expression plays a common and important role in the establishment and/or maintenance of adaxial–abaxial polarity (Juarez et al., 2004; Itoh et al., 2008a).

* Corresponding author. Fax: +81 3 5841 5064.
E-mail address: anagato@mail.ecc.u-tokyo.ac.jp (Y. Nagato).
[1] These authors contributed equally to this study.
[2] Present address: Hashie Institute for Biological Science, Kaneko Seeds Inc., Isesaki 372-0001, Japan.
[3] Present address: National Institute of Crop Science, NARO, Tsukuba, 305-8518, Japan.

0012-1606/$ – see front matter © 2009 Elsevier Inc. All rights reserved.
doi:10.1016/j.ydbio.2009.07.042

Several other mutants that affect leaf polarity and SAM initiation have been identified in monocots. For example, the *leafbladeless1* (*lbl1*) mutant in maize and the *shoot organization1* (*sho1*), *shootless2* (*shl2*), and *shl4*/*sho2* mutants in rice have mutations in key components of the *trans*-acting siRNA pathway (Timmermans et al., 1998; Satoh et al., 1999; Itoh et al., 2000; Nagasaki et al., 2007; Nogueira et al., 2007; Itoh et al., 2008b). Loss of the *trans*-acting siRNA pathway in *Arabidopsis* causes defects in phase change during vegetative development, but does not obviously affect leaf polarity (Peragine et al., 2004). The *PHANTASTICA* (*PHAN*) gene from *Antirrhinum* encodes a MYB transcription factor that is required for adaxial leaf fate determination (Waites and Hudson, 1995; Waites et al., 1998). Although a severe *phan* phenotype shows abaxialized leaves, mutation of its orthologous gene *ASYMMETRIC LEAVES1* (*AS1*) in *Arabidopsis* shows milder polarity defects (Byrne et al., 2000; Xu et al., 2003), suggesting that there are redundant pathways. ASYMMETRIC LEAVES2 (AS2) is co-localized with AS1 in subnuclear bodies, and is required for proper AS1 function (Iwakawa et al., 2002; Xu et al., 2003; Ueno et al., 2007). Several enhancer mutant screenings using the *as1* or *as2* mutant found components for *trans*-acting siRNA production, 26S proteasome subunits, and ribosomal proteins (Li et al., 2005; Garcia et al., 2006; Huang et al., 2006; Pinon et al., 2008; Yao et al., 2008). These results indicate that adaxial–abaxial leaf patterning is controlled during various regulatory steps at the RNA and protein levels.

It is important to identify the genetic components involved in leaf axis formation and proper leaf development along these axes. In this study, we show that a calpain-like cysteine proteinase is required for leaf development along the adaxial–abaxial and proximodistal axes and embryonic development through epidermal specification. Similarly, a calpain-like cysteine proteinase (phytocalpain) is essential for the development of both the epidermal cell layer and the specialized aleurone layer of the endosperm during seed development in maize, *Arabidopsis*, and tobacco (Becraft and Asuncion-Crabb, 2000; Becraft et al., 2002; Lid et al., 2002, 2005; Ahn et al., 2004; Johnson et al., 2005). A strong allele of the *defective kernel1* (*dek1*) mutant in maize causes loss of the aleurone cell layer and embryonic lethality, but homozygous mutant embryos bearing a weak allele are viable and display crinkly leaves with bulliform-like epidermal cells (Becraft et al., 2002; Lid et al., 2002). This indicates that DEK1 functions in cell-fate specification and pattern formation in the leaf epidermis. Transformants over-expressing *AtDEK1* (an orthologous gene in *Arabidopsis*) form irregular leaves that have abaxialized vasculature, whereas transformants showing a dominant negative effect through the ectopic expression of *AtDEK1* in the transmembrane region, or those subjected to RNA interference, exhibit a wide range of developmental defects, such as SAM arrest, disorganized epidermal cells, and the production of adaxialized leaves (Johnson et al., 2005; Tian et al., 2007). However, little is known regarding the relationship between phytocalpain and adaxial–abaxial axis formation.

In this study, we show that rice *adaxialized leaf1* (*adl1*) mutants containing a mutation in phytocalpain show defects in leaf polarity and SAM maintenance. Genetic and molecular approaches revealed that the *ADL1* gene may not be directly involved in establishing initial leaf polarity, but may instead affect leaf differentiation via the reception or maintenance of axis information. We also identified intermediate and strong alleles that produce shootless and globular-arrested embryos, respectively. The strong allele also resulted in partial loss of the endospermal aleurone layer on the ventral side. Moreover, epidermal markers were not expressed in the early shootless embryo. Together, these results show that various phenotypes observed in *adl1* mutants commonly exhibit defects in epidermal developmental. Tight linkage between defects in leaf pattern formation and epidermal differentiation suggest that these two processes are genetically interrelated. We propose that *ADL1* is associated with axis formation by promoting proper epidermal development in organs and embryo.

Materials and methods

Plant materials

We used eight recessive mutants of rice (*Oryza sativa* L.) derived from two independent loci: seven alleles (*adl1-1* to *adl1-3*, *adl1-s1*, *adl1-s2*, *adl1-g1*, and *adl1-g2*) at *ADL1*, and one allele (*ads*) at *ADS* (Hong et al., 1995; Sato and Kawashima, 2001). For phenotypic analyses in the vegetative phase, we mainly used *adl1-1*. All the mutants had a genetic background of cv. Taichung 65, and were obtained via chemical mutagenesis using *N*-methyl-*N*-nitrosourea (MNU). These mutations, except for *ads*, were maintained in a heterozygous state.

Histological analysis

For fresh sections, samples were embedded in 5% agar and cut with a microslicer (50-μm thick). For paraffin sections, samples were fixed in formaldehyde-acetic acid solution (formaldehyde:glacial acetic acid: ethanol = 1:1:18) for 24 h at 4 °C, dehydrated in a graded ethanol series, and embedded in Paraplast plus (McCormick Scientific). Microtome sections (8-μm thick) were stained with Delafield's hematoxylin. For plastic sections, leaf blades were fixed in formalin–acetic acid–ethanol for 24 h at 4 °C. After dehydration in a graded ethanol series, samples were embedded in Technovit 7100 (Heraeus Kulzer) and cut with a microtome. Sections were stained with toluidine blue.

Map-based cloning

To map the *ADL1* locus, *adl1-1*, *adl1-3*, and *adl1-s1* heterozygous plants (*O. sativa* L. ssp. japonica) were crossed with cv. Kasalath (ssp. indica), respectively, and siblings with abaxially curled leaves in the F2 populations of *adl1-1* and *adl1-3* and seeds with shootless embryos in that of *adl1-s1* were examined for recombination between the mutation and PCR-based polymorphic markers. The *ADL1* locus was mapped onto the long arm of chromosome 2 using STS markers obtained from the rice genome database (http://rgp.dna.affrc.go.jp/E/publicdata/caps/index.html). Further mapping delimited the *ADL1* locus in the 122.6 to 125.9 cM region between two CAPS markers. The genomic sequences of *ADL1* (TIGR's LOC_Os ID; Os02g47970 and RAP ID; Os02g0709400) in *adl1* mutants were amplified via PCR using ExTaq DNA polymerase (TaKaRa). The resulting PCR products were directly sequenced using a dye terminator cycle sequencing kit and an ABI PRISM 310 sequencer (Applied Biosystems).

In situ hybridization

Samples were fixed in 4% paraformaldehyde in 0.1 M sodium phosphate buffer for 24 h 4 °C and then dehydrated in a graded ethanol series, replaced with xylene, and embedded in Paraplast plus. Paraffin sections (8-μm thick) were applied to microscope slides coated with APS (Matsunami Glass). The *OSH1* and *ADL1* probes were prepared from the coding regions without the poly(A) region of each gene. The *RAmy1A*, *OSHB3*, and *Roc1* probes were prepared as previously described (Sugimoto et al., 1998; Ito et al., 2002; Itoh et al., 2008a). Digoxigenin (DIG)-labeled antisense and sense RNA probes were generated by transcription with T7 RNA polymerase and DIG-RNA labeling mix (Roche). *In situ* hybridization and immunological detection of the hybridization signals were carried out as described by Kouchi and Hata (1993).

Gene expression profiling

Total RNA was extracted using TRIzol reagent (Invitrogen) or RNeasy (Qiagen) according to the manufacturer's instructions. One microgram of RNA after DNase-I digestion was used for first-strand cDNA synthesis, and the RT reaction was performed using the High

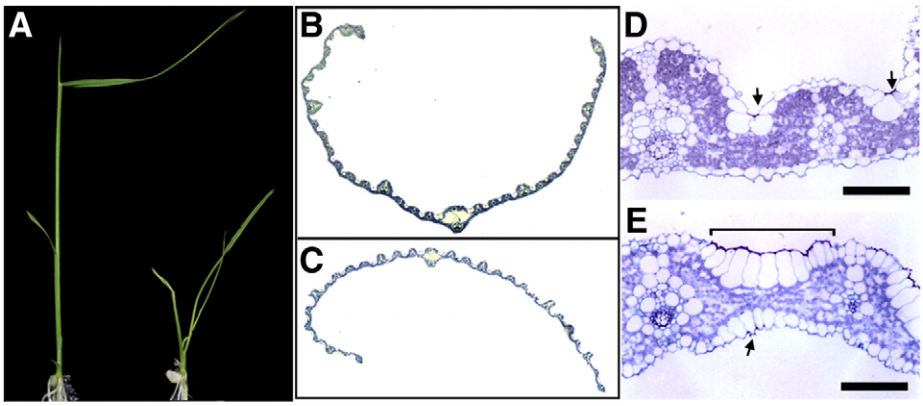

Fig. 1. Leaf phenotypes of *adl1*. (A) Seven-day-old seedlings of wild type (left) and *adl1-1* (right). (B and C) Cross sections of leaf blade in wild type (B) and *adl1-1* (C). (D and E) Cross sections of leaf blade in wild type (D) and *adl1-1* (E). Arrowheads and line segment indicate bulliform cells (D) or bulliform-like cells (E) stained dark blue with toluidine blue. Bars, 50 μm in (D and E).

Capacity RNA-to-cDNA Master Mix (Applied Biosystems). To quantify gene expression, PCR was performed using the TaqMan Fast Universal PCR Master Mix, FAM-labeled TaqMan probes for each gene (Applied Biosystems), and the StepOnePlus real-time PCR system (Applied Biosystems). The expression level of each sample was normalized against that of an internal control, *ACT1*. The primers and TaqMan probes for *OSHB1* to *OSHB5* were prepared as described by Itoh et al. (2008a). The primers for *ACT1* were 5′-GCT ATG TAC GTC GCC ATC CA-3′ and 5′-GCT GAC ACC ATC ACC AGA GT-3′, and the TaqMan probe was 5′-CAA TAC CTG TGG TAC GAC CAC TGG CAT ACA G-3′, including FAM dye at the 5′-end and BQH1 at the 3′-end.

For RT-PCR, RNA extraction was performed as described above for each tissue. Reverse-transcribed cDNA was synthesized from 5 μg of total RNA using Superscript III reverse transcriptase (Invitrogen). The primers used for amplification were: 5′-ATC TGG CTT CTT CTT TGG GG-3′ and 5′-TGC CCC TTC CTT CGA AAA CC-3′ for *ADL1* 5′-CAA TCG TGA GAA GAT GAC CC-3′ and 5′-GTC CAT CAG GAA GCT CGT AGC-3′ for *ACT1*.

Results

Isolation of the adl1 mutant

To isolate the genetic components that regulate leaf polarity and development in rice, we isolated three recessive *adl1* mutants showing apparent adaxialized leaves. Because the allelism test revealed that these mutants were allelic, we named them *adaxialized leaf 1-1* (*adl1-1*), *adl1-2*, and *adl1-3*, respectively, all of which exhibited similar phenotypes.

Effect of adl1 on leaf polarity

The *adl1* mutants were semi-dwarf with abaxially rolled leaves (Figs. 1A–C). In the wild type, the leaf blade curved adaxially (*i.e.*, adaxial surface to the inside) under drought conditions, whereas the *adl1* mutants showed abaxially curved leaves regardless of the water condition (Figs. 1B and C). Leaf rolling is mainly regulated by bulliform cells that are specifically distributed on the adaxial surface of the blade and stain dark blue with toluidine blue (TB) (Fig. 1D). In the *adl1* leaf blade, most epidermal cells on both the adaxial and abaxial sides were large and rectangular (*i.e.*, morphologically indistinguishable from bulliform cells) and cells on both sides stained dark blue in the presence of TB (Figs. 1D and E), indicating that epidermal cells in the *adl1* mutants were adaxialized.

Next, we examined whether the polarity of the internal tissue was also disrupted in *adl1* leaves. The polarity of vascular bundles was normal; xylem formed on the adaxial side, and phloem on the abaxial side (Fig. S1). Adaxialization of the mesophyll tissues was unclear because rice mesophyll cells exhibit no remarkable morphological distinction between adaxial and abaxial sides. This is in contrast to

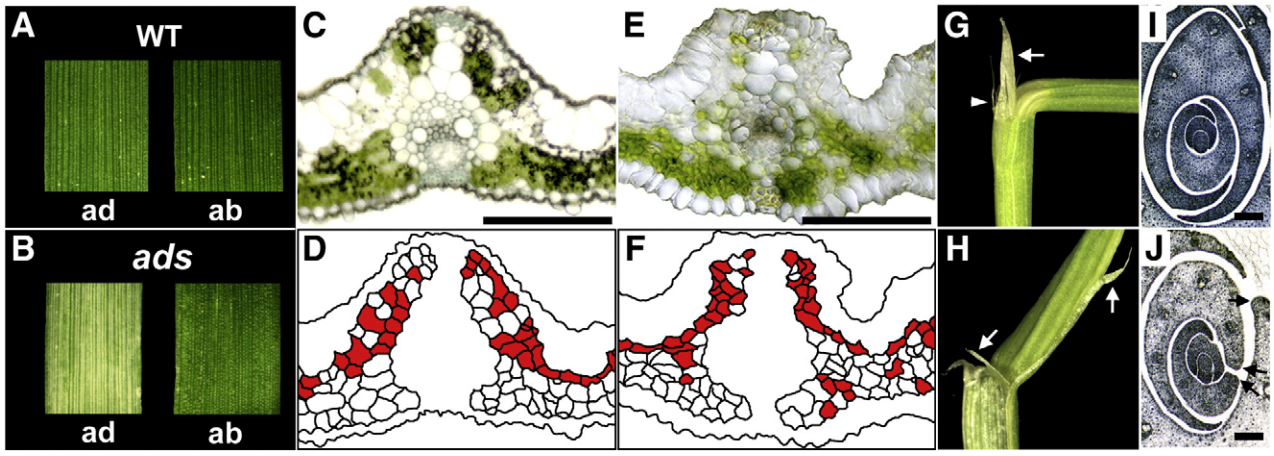

Fig. 2. The *adl1* phenotypes in leaf. (A and B) External appearance of adaxial (ad) and abaxial (ab) sides of leaf blade in wild type (WT) and *ads*. (C and E) Cross sections of fresh leaf blades of *ads* (C) and *adl1-1 ads* double mutant (E). (D and F) Schematic representation of albino cell distribution in (C) and (E), respectively. Cells painted in red indicate albino cells. (G and H) Leaf blade–sheath boundary in wild type and *adl1-1*. Arrowhead and arrows indicate auricle and ligules, respectively. (I and J) Cross sections of shoot apex in wild type (I) and *adl1-1* (J). Arrows in (J) indicate rounded leaf margin. Bars, 100 μm in (C, E, I and J).

Table 1
Frequency of albino cells in adaxial and abaxial regions of mesophyll tissue in *ads*, *adl1* and *adl1 ads*.

Leaf no.	1		2		3	
Region	Adaxial	Abaxial	Adaxial	Abaxial	Adaxial	Abaxial
ads						
Frequency of albino cells[a]	37/60 (61.67)	0/41 (0.00)	61/72 (84.72)	1/63 (0.02)	81/94 (86.17)	0/59 (0.00)
adl1-1						
Frequency of albino cells	0/80 (0.00)	0/61 (0.00)	1/75 (0.01)	0/52 (0.00)	0/123 (0.00)	0/64 (0.00)
adl1-1 ads						
Frequency of albino cells	41/69 (59.42)	10/57 (17.54)	76/131 (58.02)	10/62 (16.13)	86/123 (69.92)	25/107 (23.36)

[a] No. of albino cells/no. of cells examined.

dicots, in which mesophyll tissue differentiates into palisade or spongy tissue along the adaxial–abaxial axis. Thus, a marker mutant that could be used to discriminate between adaxial and abaxial mesophyll tissues was required. We recently isolated the *adaxial snowy leaf* (*ads*) mutant, in which the adaxial side of the leaf blade appears whitish, whereas the abaxial side is green (Figs. 2A and B). Transverse sections of fresh *ads* leaf blade revealed that many of the adaxial mesophyll cells were albino, whereas almost all the abaxial mesophyll cells remained green (Figs. 2C and D, Table 1); these results indicate that the albino cells in the *ads* leaf are a good marker of adaxial mesophyll identity. Thus, we constructed an *adl1-1 ads* double mutant. More than half of mesophyll cells in the adaxial region of the double mutant are albino as in the *ads* mutant. In the double mutant, albino cells were also distributed in the abaxial mesophyll region where no albino cells were observed in the *ads* mutant, although the frequency of albino cells in the abaxial region was lower than in the adaxial region (Figs. 2E and F, Table 1). These observations suggest that the abaxial mesophyll tissue of the *adl1* mutant has at least partially acquired adaxial identity.

Although *adl1* abnormality was most evident in leaf adaxial–abaxial polarity, other defects in leaf development were also observed. The leaves of *adl1* were shorter than those of the wild type (Table 2). In the wild type, the leaf blade–sheath boundary is formed horizontally where the ligule and auricles differentiate (Fig. 2G). In *adl1* leaves, the blade–sheath boundary was slanted, which resulted in the ligule being disrupted in the proximodistal direction (Fig. 2H). In addition, *adl1* leaves lacked auricles, which are normally formed in the margins of the blade–sheath boundary. The lack of auricles is a result of failed leaf margin establishment, which manifests as rounded margins in the *adl1* leaf sheath (in contrast to membranous margins in the wild type; Figs. 2I and J). Thus, *adl1* leaves have defects in the central–marginal polarity, as well as in the adaxial–abaxial axis.

Class III *HD-ZIP* (*HD-ZIPIII*) genes are central regulators in establishing leaf polarity. In rice, five *HD-ZIPIII* genes show conserved functions with their homologs in *Arabidopsis* (Itoh et al., 2008a). We examined the expression profile of rice *HD-ZIPIII* genes (*OSHB* genes) by *in situ* hybridization and real-time polymerase chain reaction (PCR). In the shoot apex of *adl1-1*, the expression level and patterns of the *OSHB* genes were not noticeably affected (Figs. 3A, C and D, Fig. S1). However, in mature *adl1* leaves, the expression of the *OSHB* genes was significantly enhanced (Fig. 3B). These results suggest that the *ADL1* gene might not be directly involved in setting up initial leaf polarity, but rather is associated with the maintenance of axis information.

Table 2
SAM size and leaf blade length in *adl* mutants.

Alleles	Leaf blade (mm)		SAM (μm)	
	2nd leaf	3rd leaf	Width	Height
WT	14.58 ± 0.69	70.04 ± 11.83	56.40 ± 0.76	40.56 ± 0.85
adl1-1	9.46 ± 0.79	24.00 ± 9.53	55.51 ± 5.22	22.31 ± 3.68
adl1-2	13.25 ± 0.70	36.13 ± 6.74	56.19 ± 2.55	26.26 ± 1.84
adl1-3	11.36 ± 0.44	34.93 ± 1.58	50.21 ± 2.67	23.18 ± 2.58

Each value indicates the mean of more than ten 8-day-old seedlings ± SE.

Effects of ADL1 on SAM

Because leaf primordia differentiate from the peripheral region of the SAM, we examined the *adl1* SAM (Figs. 4A and B). In the SAM, the L1 cells of the *adl1* mutant were larger than those of the wild type (Figs. 4C–E). A reduction in the height of the SAM was detected, but width was unaffected (Table 2). To confirm that this reduction in height was caused by the abnormal formation of the leaf primordium, we examined formation of the P0 leaf primordium in *adl1* plants using the *OSH1* gene, which is expressed in indeterminate cells of the SAM, but down-regulated in the P0 primordium (Fig. 4F; Sentoku et al., 1999). Down-regulation of *OSH1* was observed in more apical positions of *adl1* SAM than in the wild-type SAM (Fig. 4G). That is, leaf primordia were formed at more apical positions in the *adl1* SAM than in the wild type. These results suggest that the *ADL1* gene is involved in SAM maintenance and specification of the leaf primordium position.

ADL1 encodes the calpain-like cysteine protease

We identified the *ADL1* gene using a map-based approach with *adl1* mutants in the F_2 population between *adl1-1* heterozygotes and *indica* cv. Kasalath. The *ADL1* gene was mapped between 122.6 and 125.9 cM on chromosome 2. This region contains a putative maize *DEK1* ortholog encoding a plant-specific calpain-like cysteine protease (phytocalpain; Lid et al., 2002). Because the phenotype of the *adl1* mutant is similar to that of the *dek1-D* mutant, which is a weak allele of *DEK1* (Becraft et al., 2002), we examined the sequence of the *DEK1* ortholog in *adl1* mutants. We found mutations in this gene in all *adl1* mutants (Fig. 5A). *ADL1* is a single copy gene for rice phytocalpain and consists of a total of 21 predicted transmembrane domains, an extracellular loop domain (domain C), an intracellular domain (domain D), and a calpain-like cysteine proteinase domain (calpain domain) within 2162 amino acids (Figs. 5A and B; Lid et al., 2002). The *adl1-1* mutation caused an amino acid substitution in the calpain domain. This amino acid is conserved among phytocalpains, but not in animal calpains. The *adl1-2* mutation caused a substitution within a conserved amino acid sequence near an area that is defined as the cysteine proteinase center (Wang et al., 2003). The *adl1-3* mutant contained a single nucleotide change in the splicing acceptor site at the 5′-end of 4th exon. Reverse transcription (RT)-PCR analysis showed that unusual splicing in the *adl1-3* mutant resulted in abnormal proteins with two or four additional amino acids in the transmembrane domain (Fig. S2). Therefore, we concluded that *ADL1* encodes a phytocalpain consisting of 2162 amino acids. The amino acid identities of ADL1 to DEK1 and AtDEK were 90.1% and 58.8% in domain C, 91.1% and 71.9% in domain D, and 96.3% and 87.0% in the calpain domain, respectively.

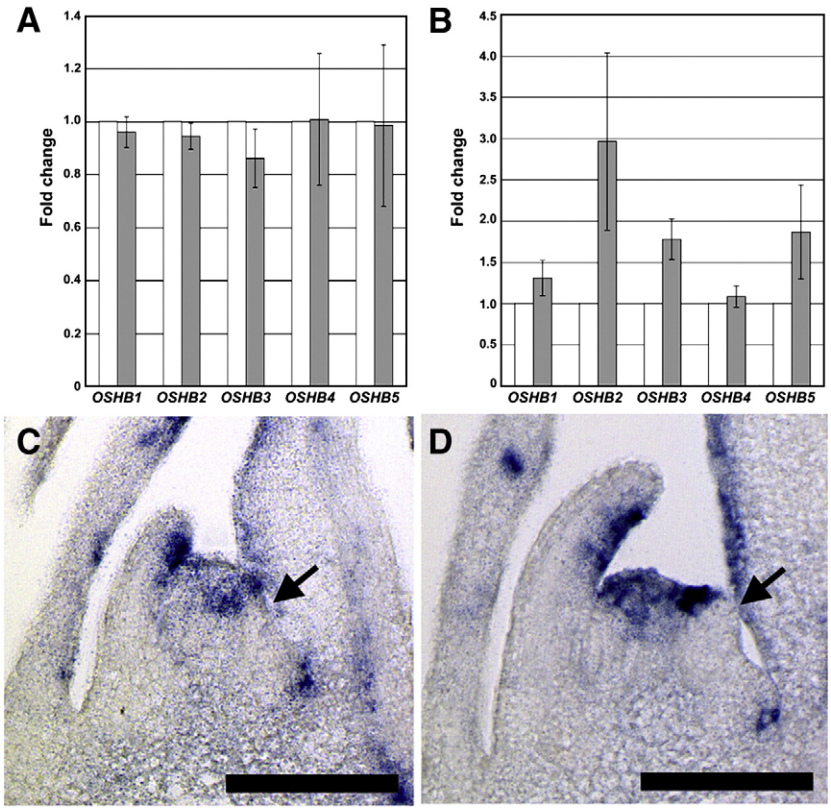

Fig. 3. Expression profiles of *OSHB* genes. Real-time RT-PCR analysis of five *OSHB* genes in the shoot apex including SAM and P1 to P3 leaf primordia (A) and the mature 2nd leaf blade (B) of wild type (white bars) and *adl1-1* (gray bars). Expression level was normalized to that of *ACT1*. Fold-change relative to wild-type plant is shown. Bars indicate standard deviation of three biological replicates. (C and D) Expression patterns of *OSHB3* gene in SAM of wild type (C) and *adl1-1* (D). Arrows indicate the P1 leaf primordia. Bars, 50 μm in (C and D).

shootless 3 is a strong adl1 allele

In rice, four mutant loci (*shootless1* [*shl1*] to *shl4*) are known to cause the deletion of the embryonic SAM and coleoptile (Hong et al., 1995; Satoh et al., 1999). One of these mutants, *shl3*, phenotypically differs from other *shl* mutants. The apical region of the *shl3* embryo, including the SAM, coleoptile, and scutellum, is almost completely deleted (Satoh et al., 1999). The *shl3* embryo showed no morphological

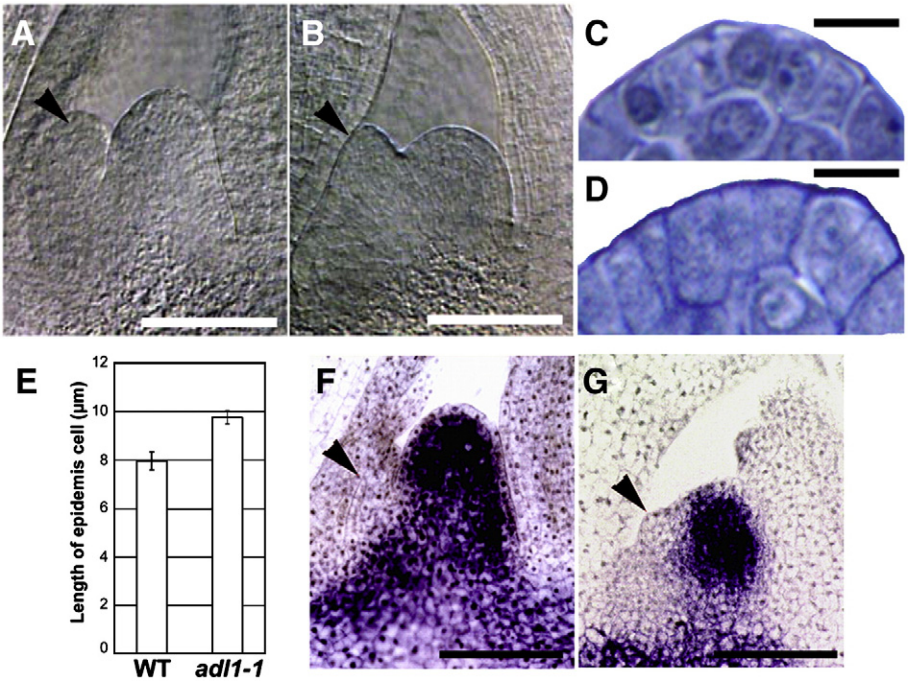

Fig. 4. *adl1* phenotypes in shoot apex. (A and B) SAM in wild type (A) and *adl1-1* (B). (C and D) Enlarged view of L1 layer of SAM in wild type (C) and *adl1-1* (D). (E) Comparison of L1 cell size in the SAM of 7-day-old wild-type and *adl1-1* seedlings. L1 cell size was measured as the length perpendicular to SAM surface using ten SAMs. Vertical bars indicate standard deviation. (F and G) *in situ* localization of *OSH1* mRNA in wild type (F) and *adl1-1* (G). Arrows indicate the P1 leaf primordia. Bars, 100 μm in (A, B, F and G) and 10 μm in (C and D).

sign of coleoptile or SAM formation at 4 days after pollination (DAP; Figs. 6A–D), and later the apical region was occupied by enlarged cells with large vacuoles. The *shl3* radicle continued to grow without dormancy, and formed a few lateral roots in the mature embryo (Fig. 6G). A few *shl3* embryos lacked a clear root structure (Fig. 6H). Interestingly, the *SHL3* locus mapped very closely to the *ADL1* locus, although the *adl1-1* to *adl1-3* embryos did not show obvious abnormalities (Figs. 6E and F). An allelism test revealed that *adl1* and *shl3* are allelic. As expected, two *shl3* mutants contained point mutations in the *ADL1* gene (Figs. 5A and B). Thus, *shl3-1* and *shl3-2* were renamed *adl1-s1* and *adl1-s2*, respectively (Table 3). The *adl1-s1* mutants caused an amino acid substitution that is conserved among phytocalpains in the calpain domain, and the *adl1-s2* mutant contained a single nucleotide substitution in the splicing acceptor site at the 5′-end of the 19th exon. RT-PCR analysis showed that the *adl1-s2* mutation resulted in various sizes of *ADL1* transcripts and produced aberrant proteins with an additional 26 amino acids in the domain D by creating a new junction between the 18th and 19th exons (Fig. S2).

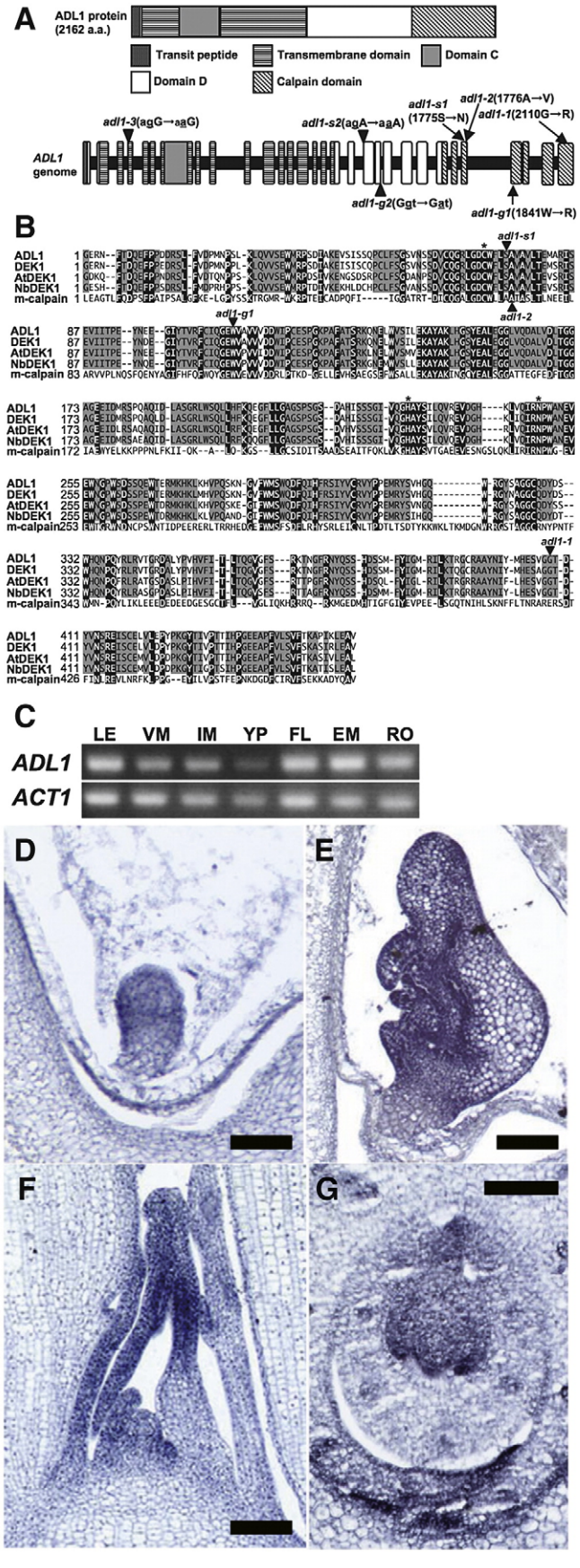

Fig. 5. *ADL1* encodes calpain-like cysteine protease. (A) Deduced ADL1 protein and *ADL1* genomic structure. *ADL1* contains 30 exons (boxes) and 29 introns (lines). Arrows and arrowheads indicate the splicing site mutations and the amino acid substitution mutations, respectively in seven *adl1* alleles. (B) Multiple sequence alignment of predicted calpain domain among ADL1 (AB477099), maize DEK1 (AAL38187), *Arabidopsis* AtDEK1 (AAL38186), tobacco NbDEK1 (AAQ55288) and human m-calpain (AAA35645). The asterisks indicate the enzyme catalytic triad residues conserved in cysteine proteinase. Arrows indicate amino acid substitution points in four *adl1* alleles. Identical residues among the four phytocalpains are highlighted in gray, and conserved residues in the four phytocalpains and m-calpain are shown in black background. (C) Semi-quantitative RT-PCR analysis of *ADL1* in different tissues. LE; leaf blades, SA; 7 day-old shoot apex, IA; inflorescence apex, YP; young panicles, FL; florets, EM; 5 DAP embryos, RO; roots. (D–G) *in situ* localization of *ADL1* transcripts in 3 DAP embryo (D), 6 DAP embryo (E), longitudinal (F) and cross (G) sections of 3-week-old shoot apex. Bars, 100 μm in (D)–(G).

Altered expression of several marker genes in the adl1 embryo

RT-PCR and *in situ* hybridization revealed that *ADL1* transcripts were detected in all tissues examined and strongly expressed in the whole embryo, vasculature, leaf primordia, leaf margins, and SAM (Figs. 5C–G). This expression pattern is consistent with abnormal phenotypes, including leaf adaxialization, deletion of leaf margins, and the apical displacement of leaf primordium insertion in the SAM. Strong expression of *ADL1* in the embryo suggests that it plays an important role in embryonic development.

Fig. 7 shows the expression of several molecular markers (*OSH1*, *OSHB3*, *ROC1*, and *RAmy1A*) in the SAM and epidermis in the *adl1-s2* embryo. *OSH1* is normally expressed in the region where the SAM and epiblast will develop (Fig. 7A). In *adl1-s2*, *OSH1* expression was observed in the ventral region of the 5 DAP embryo, where the SAM and epiblast are formed (Fig. 7B). This expression disappeared completely before 7 DAP (data not shown). To confirm whether this *OSH1* expression pattern reflects the initiation of the SAM, we examined the expression of *OSHB3*, which is essential for SAM formation and is expressed in embryonic SAM, on the adaxial side of leaf and vasculature in 5 DAP wild-type embryos (Fig. 7C). In *adl1-s2* embryos, *OSHB3* was not expressed in the ventral region, but expression in the vasculature was retained (Fig. 7D), indicating that *adl1-s2* embryos may have established the domain for SAM initiation, but failed to develop the SAM.

Next, we investigated the expression of two L1 layer markers, *ROC1* and *RAmy1A*. In the wild type, *ROC1*, an orthologus gene of *Arabidopsis ATML1*, was invariably expressed in the epidermal layer (Fig. 7E), and *RAmy1A*, a major α-amylase gene in rice, was expressed in the epithelium of the scutellum (Fig. 7F). Interestingly, both *ROC1* and *RAmy1A* expression disappeared completely in 4–5 DAP *adl1-s* embryos (Figs. 7G and H). These results indicate that the defects in epidermal development and/or its maintenance may be a major cause of the *adl1-s2* mutant phenotype.

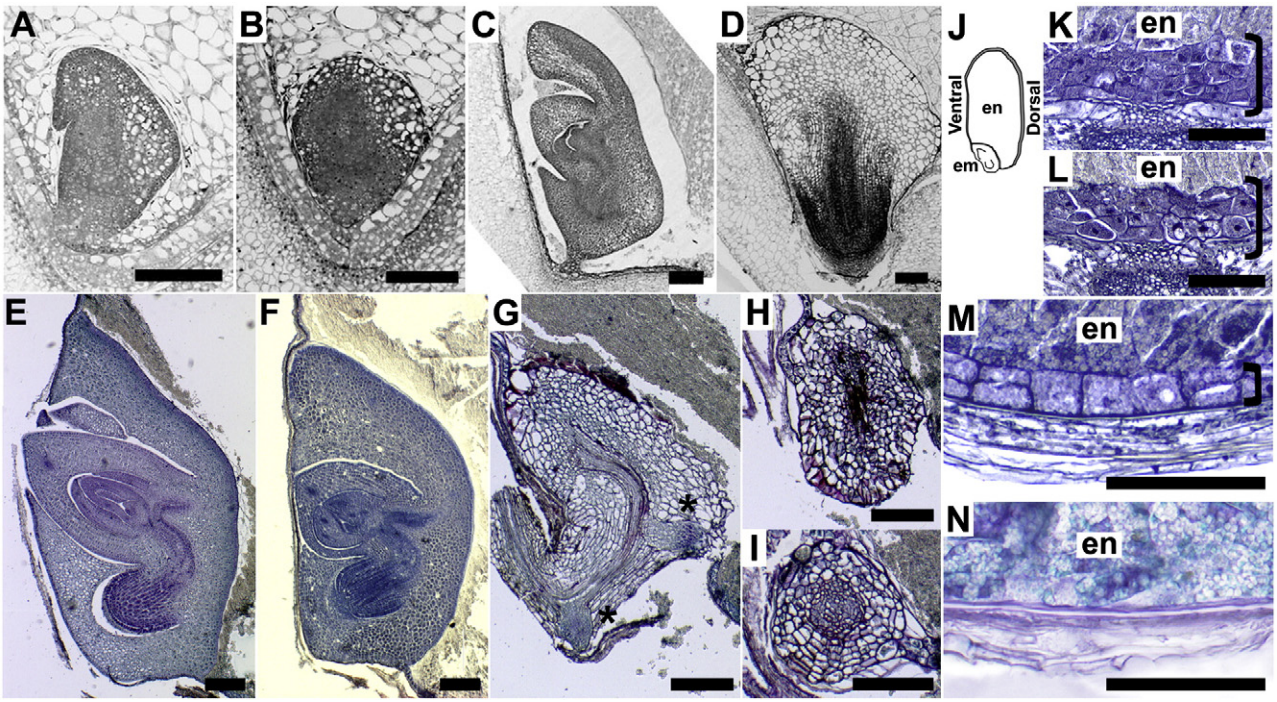

Fig. 6. Embryo and aleurone layer phenotypes in intermediate and strong *adl1* alleles. (A–D) Longitudinal sections of 4 DAP (A and B) and 7 DAP (C and D) embryos in wild type (A and C) and *adl1-s1* (B and D). (E–I) Longitudinal sections of wild type (E), *adl1-1* (F), *adl1-s2* (G and H) and *adl1-g1* (I) mature embryos. The asterisks in (G) indicate lateral roots developing precociously. (J) Schematic diagram of rice seed indicating ventral and dorsal sides. Gray line indicates aleurone layer. em; embryo, en; endosperm. (K–N) Aleurone cell layers on dorsal side (K and L) and ventral side (M and N) in wild type (K and M) and *adl1-g2* (L and N) endosperms. en; endosperm. Line segments indicate aleurone layers. Bars, 100 μm in (A)–(I) and 50 μm in (K)–(N).

Role of ADL1 in aleurone development in the endosperm

Mutations in maize *DEK1* affect the maintenance of the aleurone layer in the endosperm (Becraft and Asuncion-Crabb, 2000). The aleurone laminar structure varies among grass species. For example, there is a single-cell layer in maize and a trilaminar structure in wheat. In rice, aleurone tissue comprises 1–2 cell layers ventrally and 3–6 cell layers dorsally (Figs. 6J, K and M). Despite our expectation, the aleurone cell layers in the *adl1-s1* and *adl1-s2* mutants were normal (data not shown). It is probable that neither *adl1-s1* nor *adl1-s2* is a null allele, and that partial loss of *ADL1* function does not affect aleurone development, because the *dek1* null allele causes globular-arrested embryos (Lid et al., 2002). In order to identify alleles stronger than *adl1-s*, we screened a population of mutant embryos accumulated in our laboratory (Hong et al., 1995), and isolated two mutant lines that showed globular arrest and an abnormal aleurone layer. In these mutants, embryos failed to form any embryonic organ, but had a vasculature-like structure in the center (Fig. 6I). In addition, these mutants completely lacked the aleurone layers on the ventral side, although those on the dorsal side were normal (Figs. 6K–N). An allelism test and sequencing revealed that these mutants were allelic to *adl1*, and were designated *adl1-g1* and *adl1-g2*, respectively (Table 3). The *adl1-g1* mutant had an amino acid substitution, which is conserved in both plants and animals, in the calpain domain and *adl1-g2* contained a single nucleotide substitution in the splicing acceptor site at the 3′-end of the 20th exon. Based on RT-PCR analysis, the *adl1-g2* mutant generated a truncated protein (Fig. S2) that appeared to be unable to exert any enzymatic activity as phytocalpain, indicating that *adl1-g1* and *adl1-g2* are stronger than other alleles, and that rice phytocalpain plays an essential role in early embryonic and aleurone development.

Table 3
List of *adl1* mutant alleles.

Allele	Phenotype
adl1-1	Mild
adl1-2	Mild
adl1-3	Mild
adl1-s1 (*shl3-1*)	Intermediate
adl1-s2 (*shl3-2*)	Intermediate
adl1-g1 (*odm 63*)	Severe
adl1-g2 (*odm 78*)	Severe

Discussion

In this study, we identified the *ADL1* gene, which encodes a calpain-like cysteine proteinase and plays important roles in various developmental processes such as leaf axis formation, epidermal specification, SAM maintenance, and embryonic development. Interestingly, *adl1* mutants exhibit a considerably wide range of loss-of-function phenotypes, depending on the allele. Weak alleles (*adl1-1* to *adl1-3*) showed defects in leaf polarity and in the position of leaf primordium insertion in the SAM. Intermediate alleles (*adl1-s*) produced shootless embryos, probably due to the deletion of the apical embryonic region. In the strong alleles (*adl1-g*), embryos stop growing at the globular stage, and the endosperm lacked the aleurone cell layer on the ventral side. This study provided new insights into leaf, embryo, and aleurone development in rice.

The role of ADL1 gene in leaf development

The *adl1* leaf blades showed ectopic bulliform-like cells in the abaxial epidermis. In addition, *adl1 ads* double mutant analysis showed that internal mesophyll tissue was also adaxialized in the *adl1* mutant, suggesting that *adl1* leaves were adaxialized at least partially. In accordance with our results, transformants with dominant negative effects due to the ectopic expression of *AtDEK1* in the transmembrane

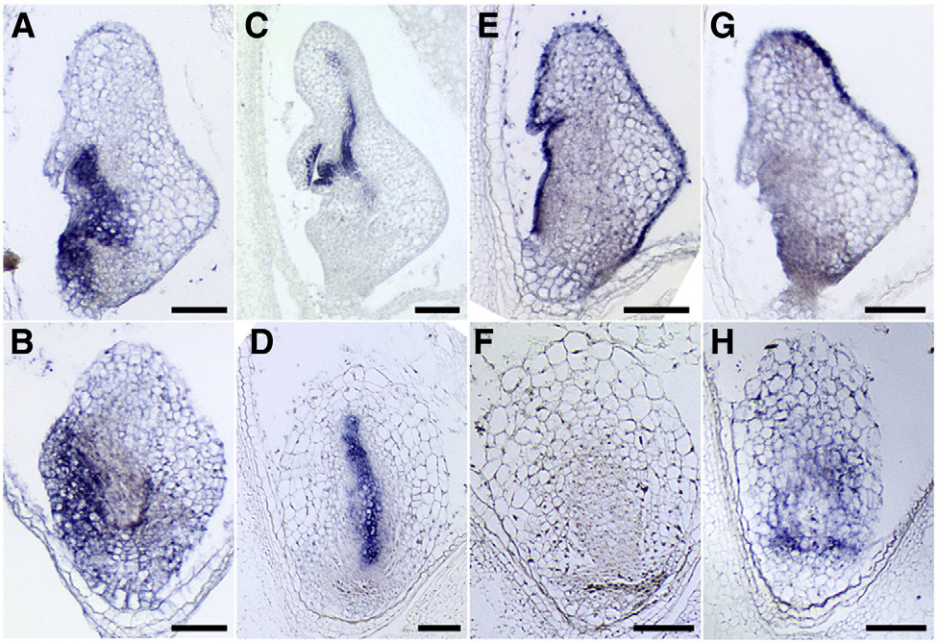

Fig. 7. Gene expression patterns of SAM and epidermis-associated genes in *adl1-s2* embryos. Expression patterns of *OSH1* (A and B), *OSHB3* (C and D), *Roc1* (E and F) and *RAmy1A* (G and H) in wild-type embryos (A, C, E and G) and *adl1-s2* embryos (B, D, F and H). (A and G); 4 DAP embryos. (B–F, H); 5 DAP embryos. Bars, 100 μm.

region or RNA interference exhibited a gradient of developmental defects, such as SAM arrest, disorganized epidermal cells, and adaxialized leaves in *Arabidopsis* (Johnson et al., 2005; Tian et al., 2007). In contrast, transformants over-expressing *AtDEK1* displayed leaves with disturbed dorsoventral patterns, including abaxialized vasculature (Lid et al., 2005). Phytocalpains have a remarkable degree of sequence conservation among angiosperms, gymnosperms, and even mosses (Margis and Margis-Pinheiro, 2003; Tian et al., 2007). Thus, it is possible that phytocalpains have a conserved role in regulating dorsoventral patterning in organs across lineages.

Other adaxial identity genes have been recently isolated in some species. *OSHB* genes, which are members of the Class III *HD-ZIP* gene family in rice, have been characterized (Itoh et al., 2008a). We evaluated the adaxialization of the *adl1* mutant using these molecular markers. The enhanced expression of *OSHB* genes in mature *adl1* leaves, but not in immature leaves, suggests that the *ADL1* gene may be involved in the maintenance of the adaxial–abaxial axis rather than in the establishment of the axis in incipient primordia.

The membrane-tethered transcription factor NTM1 has been identified as a putative target for AtDEK1 in *Arabidopsis* (Kim et al., 2006). The process for NTM1 release from the membrane and activation was differentially inhibited by the calpain inhibitor ALLN, suggesting that NTM1 may be released from the membrane through AtDEK1 calpain activity. It was demonstrated that the activation of membrane-bound transcription factors through proteolytic cleavage is mediated via one of two distinct processes: regulated intramembrane proteolysis (RIP) or regulated ubiquitin/26S proteasome-dependent processing (RUP). In RIP, active transcription factors are liberated by specific membrane-associated proteases (Vik and Rine, 2000; Hoppe et al., 2001). In RUP, pre-transcription factors are ubiquitinated and degraded by the 26S proteasome in a controlled manner, resulting in the release of transcriptionally active forms. Interestingly, mutations in the subunits of the 26S proteasome in *Arabidopsis*, such as *AE3/RPN8a*, strongly enhanced the polarity defects in *as1* or *as2* leaves and caused the abaxialization of leaves (Huang et al., 2006). Thus, proteolysis-mediated liberation of active membrane-bound transcription factors through phytocalpain or 26S proteasome could be cooperatively involved in the establishment of adaxial–abaxial polarity.

Several *adl1* alleles have amino acid substitutions that are conserved only in phytocalpains, revealing important information regarding plant-specific phytocalpain function. Johnson et al. (2008) reported that *AtDEK1* undergoes autolytic cleavage within plant-specific domain D and at the start of the calpain domain. In addition, only the calpain domain is able to fully complement the embryonic lethal phenotype in the *atdek1* mutant, suggesting the possibility that domains other than the calpain domain are involved in the regulation of calpain activation. We showed in this study that the *adl1-3* protein has a defect in the transmembrane region and the *adl1-s2* protein has an additional 26 amino acids in domain D due to mutation in the splicing donor site. The *adl1-3* and *adl1-s2* phenotypes are remarkably similar to *adl1-1* and *adl1-s1*, respectively, which have a substitution in the calpain domain. These results indicate that other domains, such as the transmembrane domain and domain D, are necessary for full ADL1 function.

Role of ADL1 in epidermal specification and embryogenesis

Weak *adl1* alleles simultaneously showed aberrant axis formation in leaves and abnormal epidermal cells in leaves and the SAM. Intermediate *adl1-s* embryos lacked the apical region and epidermal identity. Defects in embryonic axis formation and epidermal cell identity were also observed in strong *adl1-g* alleles.

The tight linkage observed between defects in axis formation and epidermal differentiation in *adl1* suggests that these two processes are interrelated. Recently, the role of the epidermis in shoot development and embryogenesis was discussed. In the tomato, laser ablation of the meristem L1 layer resulted in a gradual degeneration of SAM activities, and in the production of partially or entirely radialized leaf primordia (Reinhardt et al., 2003, 2005). Two receptor-like kinases, TOAD2 and RPK1, are redundantly required for both the maintenance of protoderm specification and subprotoderm differentiation in radial pattern formation in the *Arabidopsis* embryo (Nodine et al., 2007). In addition, Savaldi-Goldstein et al. (2007) showed that dwarfism caused by *bri1* could be rescued by expressing the *BRI1* gene only in the epidermal layer. Consequently, they suggested that the epidermal layer controls the development of inner tissues. Taking all of these results into consideration, *ADL1* may be associated with

axis formation by promoting proper epidermal development in organs and the embryo. Further research on the identification of potential ADL1 targets and investigation of tissue-specific ADL1 function will help to elucidate the relationship between the epidermis and adaxial–abaxial axis formation.

Acknowledgments

We thank Noboru Washizu, Ken-ichiro Ichikawa, Ryuichi Soga, and Keisuke Yatsuda for their assistance in cultivating rice plants at the Experimental Farm of the University of Tokyo. This work was supported in part by Grants-in-Aid for Scientific Research from the Ministry of Education, Culture, Sports, Science, and Technology of Japan (20248001 to Y.N. and 20061005 to J.-I.I.). K.H. was supported by a grant from the Japan Society for the Promotion of Science Research Fellowship for Young Scientists.

Appendix A. Supplementary data

Supplementary data associated with this article can be found, in the online version, at doi:10.1016/j.ydbio.2009.07.042.

References

Ahn, J.W., Kim, M., Lim, J.H., Kim, G.T., Pai, H.S., 2004. Phytocalpain controls the proliferation and differentiation fates of cells in plant organ development. Plant J. 38, 969–981.

Becraft, P.W., Asuncion-Crabb, Y., 2000. Positional cues specify and maintain aleurone cell fate in maize endosperm development. Development 127, 4039–4048.

Becraft, P.W., Li, K., Dey, N., Asuncion-Crabb, Y., 2002. The maize *dek1* gene functions in embryonic pattern formation and cell fate specification. Development 129, 5217–5225.

Bowman, J.L., Eshed, Y., Baum, S.F., 2002. Establishment of polarity in angiosperm lateral organs. Trends Genet. 18, 134–141.

Byrne, M.E., Barley, R., Curtis, M., Arroyo, J.M., Dunham, M., Hudson, A., Martienssen, R.A., 2000. *Asymmetric leaves1* mediates leaf patterning and stem cell function in *Arabidopsis*. Nature 408, 967–971.

Chitwood, D.H., Guo, M., Nogueira, F.T., Timmermans, M.C., 2007. Establishing leaf polarity: the role of small RNAs and positional signals in the shoot apex. Development 134, 813–823.

Emery, J.F., Floyd, S.K., Alvarez, J., Eshed, Y., Hawker, N.P., Izhaki, A., Baum, S.F., Bowman, J.L., 2003. Radial patterning of *Arabidopsis* shoots by class III HD-ZIP and KANADI genes. Curr. Biol. 13, 1768–1774.

Eshed, Y., Izhaki, A., Baum, S.F., Floyd, S.K., Bowman, J.L., 2004. Asymmetric leaf development and blade expansion in *Arabidopsis* are mediated by KANADI and YABBY activities. Development 131, 2997–3006.

Garcia, D., Collier, S.A., Byrne, M.E., Martienssen, R.A., 2006. Specification of leaf polarity in *Arabidopsis* via the *trans*-acting siRNA pathway. Curr. Biol. 16, 933–938.

Hong, S.K., Aoki, T., Kitano, H., Satoh, H., Nagato, Y., 1995. Phenotypic diversity of 188 rice embryo mutants. Dev. Genet. 16, 298–310.

Hoppe, T., Rape, M., Jentsch, S., 2001. Membrane-bound transcription factors: regulated release by RIP or RUP. Curr. Opin. Cell Biol. 13, 344–348.

Huang, W., Pi, L., Liang, W., Xu, B., Wang, H., Cai, R., Huang, H., 2006. The proteolytic function of the *Arabidopsis* 26S proteasome is required for specifying leaf adaxial identity. Plant Cell 18, 2479–2492.

Ito, M., Sentoku, N., Nishimura, A., Hong, S.K., Sato, Y., Matsuoka, M., 2002. Position dependent expression of *GL2-type* homeobox gene, *Roc1*: significance for protoderm differentiation and radial pattern formation in early rice embryogenesis. Plant J. 29, 497–507.

Itoh, J., Kitano, H., Matsuoka, M., Nagato, Y., 2000. *SHOOT ORGANIZATION* genes regulate shoot apical meristem organization and the pattern of leaf primordium initiation in rice. Plant Cell 12, 2161–2174.

Itoh, J., Hibara, K., Sato, Y., Nagato, Y., 2008a. Developmental role and auxin responsiveness of class III homeodomain leucine zipper gene family members in rice. Plant Physiol. 147, 1960–1975.

Itoh, J., Sato, Y., Nagato, Y., 2008b. The *SHOOT ORGANIZATION2* gene coordinates leaf domain development along the central–marginal axis in rice. Plant Cell Physiol. 49, 1226–1236.

Iwakawa, H., Ueno, Y., Semiarti, E., Onouchi, H., Kojima, S., Tsukaya, H., Hasebe, M., Soma, T., Ikezaki, M., Machida, C., Machida, Y., 2002. The *ASYMMETRIC LEAVES2* gene of *Arabidopsis thaliana*, required for formation of a symmetric flat leaf lamina, encodes a member of a novel family of proteins characterized by cysteine repeats and a leucine zipper. Plant Cell Physiol. 43, 467–478.

Johnson, K.L., Degnan, K.A., Ross Walker, J., Ingram, G.C., 2005. *AtDEK1* is essential for specification of embryonic epidermal cell fate. Plant J. 44, 114–127.

Johnson, K.L., Faulkner, C., Jeffree, C.E., Ingram, G.C., 2008. The phytocalpain defective kernel 1 is a novel *Arabidopsis* growth regulator whose activity is regulated by proteolytic processing. Plant Cell 20, 2619–2630.

Juarez, M.T., Kui, J.S., Thomas, J., Heller, B.A., Timmermans, M.C., 2004. microRNA-mediated repression of *rolled leaf1* specifies maize leaf polarity. Nature 428, 84–88.

Kim, Y.S., Kim, S.G., Park, J.E., Park, H.Y., Lim, M.H., Chua, N.H., Park, C.M., 2006. A membrane-bound NAC transcription factor regulates cell division in *Arabidopsis*. Plant Cell 18, 3132–3144.

Kouchi, H., Hata, S., 1993. Isolation and characterization of novel nodulin cDNAs representing genes expressed at early stages of soybean nodule development. Mol. Gen. Genet. 238, 106–119.

Li, H., Xu, L., Wang, H., Yuan, Z., Cao, X., Yang, Z., Zhang, D., Xu, Y., Huang, H., 2005. The putative RNA-dependent RNA polymerase *RDR6* acts synergistically with *ASYMMETRIC LEAVES1* and *2* to repress *BREVIPEDICELLUS* and microRNA165/166 in *Arabidopsis* leaf development. Plant Cell 17, 2157–2171.

Lid, S.E., Gruis, D., Jung, R., Lorentzen, J.A., Ananiev, E., Chamberlin, M., Niu, X., Meeley, R., Nichols, S., Olsen, O.A., 2002. The *defective kernel 1* (*dek1*) gene required for aleurone cell development in the endosperm of maize grains encodes a membrane protein of the calpain gene superfamily. Proc. Natl. Acad. Sci. U. S. A. 99, 5460–5465.

Lid, S.E., Olsen, L., Nestestog, R., Aukerman, M., Brown, R.C., Lemmon, B., Mucha, M., Opsahl-Sorteberg, H.G., Olsen, O.A., 2005. Mutation in the *Arabidopsis thaliana* DEK1 calpain gene perturbs endosperm and embryo development while over-expression affects organ development globally. Planta 221, 339–351.

Margis, R., Margis-Pinheiro, M., 2003. Phytocalpains: orthologous calcium-dependent cysteine proteinases. Trends Plant Sci. 8, 58–62.

McConnell, J.R., Barton, M.K., 1998. Leaf polarity and meristem formation in *Arabidopsis*. Development 125, 2935–2942.

McConnell, J.R., Emery, J., Eshed, Y., Bao, N., Bowman, J., Barton, M.K., 2001. Role of *PHABULOSA* and *PHAVOLUTA* in determining radial patterning in shoots. Nature 411, 709–713.

Nagasaki, H., Itoh, J., Hayashi, K., Hibara, K., Satoh-Nagasawa, N., Nosaka, M., Mukouhata, M., Ashikari, M., Kitano, H., Matsuoka, M., Nagato, Y., Sato, Y., 2007. The small interfering RNA production pathway is required for shoot meristem initiation in rice. Proc. Natl. Acad. Sci. U. S. A. 104, 14867–14871.

Nodine, M.D., Yadegari, R., Tax, F.E., 2007. *RPK1* and *TOAD2* are two receptor-like kinases redundantly required for *Arabidopsis* embryonic pattern formation. Dev. Cell 12, 943–956.

Nogueira, F.T., Madi, S., Chitwood, D.H., Juarez, M.T., Timmermans, M.C., 2007. Two small regulatory RNAs establish opposing fates of a developmental axis. Genes Dev. 21, 750–755.

Ochando, I., Jover-Gil, S., Ripoll, J.J., Candela, H., Vera, A., Ponce, M.R., Martinez-Laborda, A., Micol, J.L., 2006. Mutations in the microRNA complementarity site of the *INCURVATA4* gene perturb meristem function and adaxialize lateral organs in *Arabidopsis*. Plant Physiol. 141, 607–619.

Peragine, A., Yoshikawa, M., Wu, G., Albrecht, H.L., Poethig, R.S., 2004. *SGS3* and *SGS2*/*SDE1*/*RDR6* are required for juvenile development and the production of *trans*-acting siRNAs in *Arabidopsis*. Genes Dev. 18, 2368–2379.

Pinon, V., Etchells, J.P., Rossignol, P., Collier, S.A., Arroyo, J.M., Martienssen, R.A., Byrne, M.E., 2008. Three *PIGGYBACK* genes that specifically influence leaf patterning encode ribosomal proteins. Development 135, 1315–1324.

Prigge, M.J., Otsuga, D., Alonso, J.M., Ecker, J.R., Drews, G.N., Clark, S.E., 2005. Class III homeodomain-leucine zipper gene family members have overlapping, antagonistic, and distinct roles in *Arabidopsis* development. Plant Cell 17, 61–76.

Reinhardt, D., Frenz, M., Mandel, T., Kuhlemeier, C., 2003. Microsurgical and laser ablation analysis of interactions between the zones and layers of the tomato shoot apical meristem. Development 130, 4073–4083.

Reinhardt, D., Frenz, M., Mandel, T., Kuhlemeier, C., 2005. Microsurgical and laser ablation analysis of leaf positioning and dorsoventral patterning in tomato. Development 132, 15–26.

Reinhart, B.J., Weinstein, E.G., Rhoades, M.W., Bartel, B., Bartel, D.P., 2002. MicroRNAs in plants. Genes Dev. 16, 1616–1626.

Rhoades, M.W., Reinhart, B.J., Lim, L.P., Burge, C.B., Bartel, B., Bartel, D.P., 2002. Prediction of plant microRNA targets. Cell 110, 513–520.

Sato, K., Kawashima, S., 2001. Calpain function in the modulation of signal transduction molecules. Biol. Chem. 382, 743–751.

Satoh, N., Hong, S.K., Nishimura, A., Matsuoka, M., Kitano, H., Nagato, Y., 1999. Initiation of shoot apical meristem in rice: characterization of four *SHOOTLESS* genes. Development 126, 3629–3636.

Savaldi-Goldstein, S., Peto, C., Chory, J., 2007. The epidermis both drives and restricts plant shoot growth. Nature 446, 199–202.

Sentoku, N., Sato, Y., Kurata, N., Ito, Y., Kitano, H., Matsuoka, M., 1999. Regional expression of the rice *KN1*-type homeobox gene family during embryo, shoot, and flower development. Plant Cell 11, 1651–1664.

Sugimoto, N., Takeda, G., Nagato, Y., Yamaguchi, J., 1998. Temporal and spatial expression of the alpha-amylase gene during seed germination in rice and barley. Plant Cell Physiol. 39, 323–333.

Sussex, I.M., 1951. Experiments on the cause of dorsiventrality in leaves. Nature 167, 651–652.

Tang, G., Reinhart, B.J., Bartel, D.P., Zamore, P.D., 2003. A biochemical framework for RNA silencing in plants. Genes Dev. 17, 49–63.

Tian, Q., Olsen, L., Sun, B., Lid, S.E., Brown, R.C., Lemmon, B.E., Fosnes, K., Gruis, D.F., Opsahl-Sorteberg, H.G., Otegui, M.S., Olsen, O.A., 2007. Subcellular localization and functional domain studies of DEFECTIVE KERNEL1 in maize and *Arabidopsis* suggest a model for aleurone cell fate specification involving CRINKLY4 and SUPERNUMERARY ALEURONE LAYER1. Plant Cell 19, 3127–3145.

Timmermans, M.C., Schultes, N.P., Jankovsky, J.P., Nelson, T., 1998. *Leafbladeless1* is required for dorsoventrality of lateral organs in maize. Development 125, 2813–2823.

Ueno, Y., Ishikawa, T., Watanabe, K., Terakura, S., Iwakawa, H., Okada, K., Machida, C., Machida, Y., 2007. Histone deacetylases and ASYMMETRIC LEAVES2 are involved in the establishment of polarity in leaves of *Arabidopsis*. Plant Cell 19, 445–457.

Vik, A., Rine, J., 2000. Membrane biology: membrane-regulated transcription. Curr. Biol. 10, R869–871.

Waites, R., Hudson, A., 1995. *phantastica*: a gene required for dorsoventrality of leaves in *Antirrhinum majus*. Development 121, 2143–2154.

Waites, R., Selvadurai, H.R., Oliver, I.R., Hudson, A., 1998. The *PHANTASTICA* gene encodes a MYB transcription factor involved in growth and dorsoventrality of lateral organs in *Antirrhinum*. Cell 93, 1923–1931.

Wang, C., Barry, J.K., Min, Z., Tordsen, G., Rao, A.G., Olsen, O.A., 2003. The calpain domain of the maize DEK1 protein contains the conserved catalytic triad and functions as a cysteine proteinase. J. Biol. Chem. 278, 34467–34474.

Xu, L., Xu, Y., Dong, A., Sun, Y., Pi, L., Xu, Y., Huang, H., 2003. Novel *as1* and *as2* defects in leaf adaxial–abaxial polarity reveal the requirement for *ASYMMETRIC LEAVES1* and *2* and *ERECTA* functions in specifying leaf adaxial identity. Development 130, 4097–4107.

Yao, Y., Ling, Q., Wang, H., Huang, H., 2008. Ribosomal proteins promote leaf adaxial identity. Development 135, 1325–1334.

Zhong, R., Ye, Z.H., 2004. *amphivasal vascular bundle 1*, a gain-of-function mutation of the *IFL1*/*REV* gene, is associated with alterations in the polarity of leaves, stems and carpels. Plant Cell Physiol. 45, 369–385.